Identifying Neuroimaging Markers of Motor Disability in Acute Stroke by Machine Learning Techniques

ARTICLE *in* CEREBRAL CORTEX · MAY 2014

Impact Factor: 8.67 · DOI: 10.1093/cercor/bhu100 · Source: PubMed

Anne K Rehme
University of Cologne

Delia-Lisa Feis
Max Planck Institute for Metabolism Resear…

Thomas Liebig
University of Cologne

Simon B Eickhoff
Heinrich-Heine-Universität Düsseldorf

Cerebral Cortex Advance Access published May 16, 2014

Cerebral Cortex
doi:10.1093/cercor/bhu100

Identifying Neuroimaging Markers of Motor Disability in Acute Stroke by Machine Learning Techniques

A. K. Rehme[1,2,4], L. J. Volz[1,2], D.-L. Feis[1], I. Bomilcar-Focke[1], T. Liebig[3], S. B. Eickhoff[4,5], G. R. Fink[2,4] and C. Grefkes[1,2,4]

[1]Max Planck Institute for Neurological Research, Cologne, Germany, [2]Department of Neurology and, [3]Department of Radiology and Neuroradiology, University of Cologne, Cologne, Germany, [4]Institute of Neuroscience and Medicine (INM-2, INM-3), Research Centre Juelich, Juelich, Germany and [5]Institute of Clinical Neuroscience and Medical Psychology, Heinrich Heine University, Düsseldorf, Germany

*Address correspondence to Anne K. Rehme, Max Planck Institute for Neurological Research, Neuromodulation and Neurorehabilitation, Gleueler Str. 50, 50931 Cologne, Germany. Email: anne.rehme@nf.mpg.de

Conventional mass-univariate analyses have been previously used to test for group differences in neural signals. However, machine learning algorithms represent a multivariate decoding approach that may help to identify neuroimaging patterns associated with functional impairment in "individual" patients. We investigated whether fMRI allows classification of individual motor impairment after stroke using support vector machines (SVMs). Forty acute stroke patients and 20 control subjects underwent resting-state fMRI. Half of the patients showed significant impairment in hand motor function. Resting-state connectivity was computed by means of whole-brain correlations of seed time-courses in ipsilesional primary motor cortex (M1). Lesion location was identified using diffusion-weighted images. These features were used for linear SVM classification of unseen patients with respect to motor impairment. SVM results were compared with conventional mass-univariate analyses. Resting-state connectivity classified patients with hand motor deficits compared with controls and nonimpaired patients with 82.6–87.6% accuracy. Classification was driven by reduced interhemispheric M1 connectivity and enhanced connectivity between ipsilesional M1 and premotor areas. In contrast, lesion location provided only 50% sensitivity to classify impaired patients. Hence, resting-state fMRI reflects behavioral deficits more accurately than structural MRI. In conclusion, multivariate fMRI analyses offer the potential to serve as markers for endophenotypes of functional impairment.

Keywords: diagnostic imaging, diffusion imaging, ischemia, motor impairment, support vector machine

Introduction

Stroke is a leading cause of permanent motor disability with an incidence of >15 million people worldwide (World Health Organization 2004; Go et al. 2013). Neuroimaging techniques including structural and functional MRI (fMRI) have shown that motor deficits after stroke are associated with disturbances in anatomical pathways and brain activation patterns (Chollet et al. 1991; Ward et al. 2003, 2006; Stinear et al. 2007; Grefkes et al. 2008; Rehme, Fink et al. 2011; Rehme et al. 2012). Recent studies examined stroke-induced changes in functional connectivity between brain areas based on resting-state fMRI (Friston 1994; Rehme and Grefkes 2013; Grefkes and Fink 2014). Resting-state functional connectivity is usually determined by correlating regional low-frequency blood oxygenation level-dependent time-series assessed in the absence of an active task (Friston 1994). Resting-state studies after stroke provided evidence for a close relationship between disturbed functional connectivity of cortical motor areas distant from the lesion site and motor impairment. In particular, interhemispheric resting-state connectivity between primary motor area (M1) of both hemispheres has been shown to be reduced in stroke patients with motor impairments (Carter et al. 2010, 2012; Wang et al. 2010; Park et al. 2011; Golestani et al. 2013).

To date, neuroimaging studies in stroke research have frequently used conventional mass-univariate analyses within the framework of the General Linear Model (GLM) focusing on the statistical relationship between behavioral performance or group membership and neural signals (Friston et al. 1995). These mass-univariate analyses represent a special form of encoding models explaining how the signal measured at a given voxel is generated by underlying hidden factors (e.g., sensory, cognitive, or motor processes) based on experimental manipulations or clinical groups (Kay and Gallant 2009; Naselaris et al. 2011). Statistical inference in encoding models is thus drawn from forward models using experimental information to predict brain activity (Haufe et al. 2014). However, classical encoding analyses do not provide neuroimaging markers that can be used for the diagnosis and prognosis of functional impairment in individual patients (Orrù et al. 2012). In contrast, decoding approaches use brain activity to discriminate groups or experimental conditions (Kay et al. 2008; Kriegeskorte 2011; Naselaris et al. 2011). Here, statistical inference is based on a backward model as the data-generating process is reversed to predict experimental categories from measured brain signals (Naselaris et al. 2011; Haufe et al. 2014). Thus, decoding models test how phenotypical information can be decoded from neuroimaging data (Haufe et al. 2014). Importantly, decoding models allow classifying at the level of individual subjects. In contrast to conventional GLMs, multivariate analyses also consider voxelwise signal dependencies, which increase the power to detect signals of interest (Lemm et al. 2011; Haufe et al. 2014). This raises the clinically relevant question whether a multivariate decoding approach considering the combined multivoxel information from neuroimaging data may be used to classify behavioral performance at the level of individual patients (Orrù et al. 2012).

Support vector machines (SVMs) represent a multivariate decoding technique, which has recently been introduced into the field of clinical neuroimaging (Cortes and Vapnik 1995; Pereira et al. 2009; Lemm et al. 2011; Orrù et al. 2012). SVMs are supervised machine learning algorithms that are most commonly used for classification but can also be applied, for example, in regression analyses (Pereira et al. 2009; Chang and Lin 2011; Lemm et al. 2011; Naselaris et al. 2011). Technically, SVMs consist of a training step where data are nonlinearly mapped into a high-dimensional feature space to optimize a separation boundary between predefined classes. After training, the trained classifier is used to predict the class level of previously unseen data (Cortes and Vapnik 1995; Lemm et al. 2011; Orrù et al. 2012).

Previous studies showed that SVM analyses of resting-state fMRI data can distinguish neuropsychiatric patients from healthy controls for diseases including mild cognitive impairment, multiple sclerosis, major depression, or schizophrenia (Shen et al. 2010; Richiardi et al. 2012; Wee et al. 2012; Zeng et al. 2012). Furthermore, there is evidence that SVM techniques for task-based fMRI data may be used to predict the functional outcome of stroke patients with aphasia (Saur et al. 2010). The use of task-based fMRI in a clinical setting is, however, difficult because it requires both a sophisticated technical set-up and a sufficiently high compliance of the patient. In contrast, resting-state fMRI can be acquired within a few minutes with minimum cooperation of the patient. Therefore, classification of clinical populations based on resting-state data offers potential for providing noninvasive diagnostic markers to predict individual outcome and treatment effects in a standard clinical environment.

The aim of this study was to identify endophenotypes of motor disability after stroke by decoding motor outcome from individual resting-state fMRI connectivity patterns using SVM. Furthermore, we computed mass-univariate decoding analyses to test whether multivariate classification is superior to univariate classification (Kriegeskorte 2011; Lemm et al. 2011; Naselaris et al. 2011). To this end, we implemented a resting-state fMRI scan into a standard MRI stroke protocol and examined 3 groups: acute stroke patients with hand motor deficits, acute stroke patients without hand motor deficits, and nonstroke neurological control patients. We computed the resting-state functional connectivity of ipsilesional M1 and trained linear two-class SVMs to 1) classify new patients and 2) identify resting-state neuroimaging markers of motor deficits after stroke. Individual resting-state markers of motor impairment were compared with the results of a conventional univariate group analysis of resting-state connectivity. Finally, we also classified motor impairment based on the size and location of structural lesions to compare the sensitivity of structural and functional MRI scans.

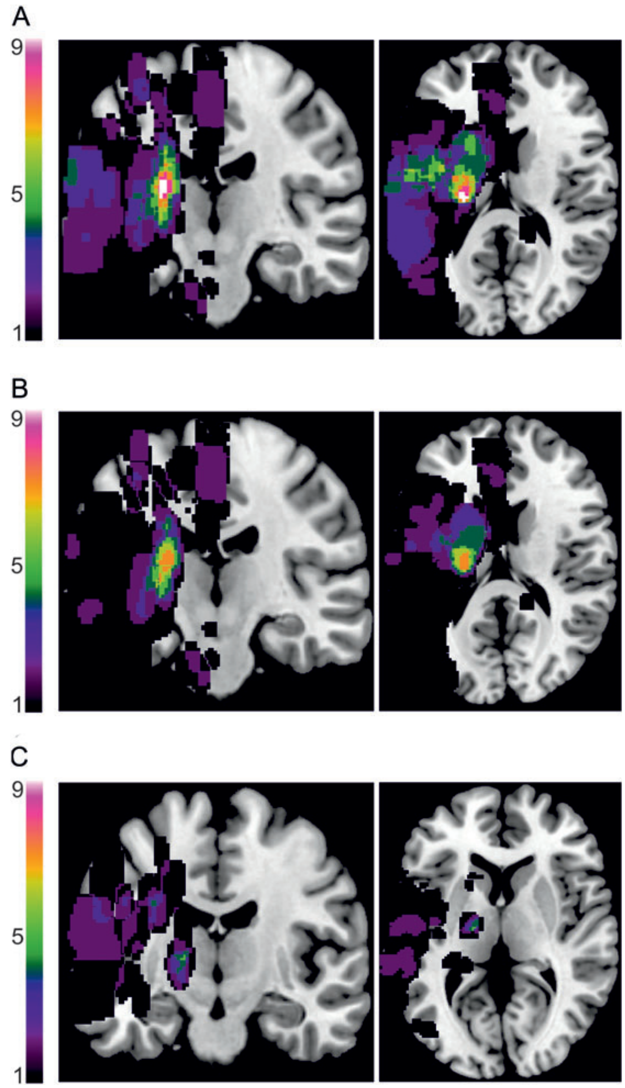

Figure 1. Summary map of DWI lesions. (*A*) For the entire sample of stroke patients, the maximum overlap (n = 9/40) was at the posterior limb of the internal capsule of the CST. (*B*) Considering each stroke group separately, the maximum overlap in patients with hand motor deficits (n = 7/20) was also found at the posterior limb of the internal capsule. Thus, the overlap of lesion locations causing hand motor deficits was rather low. (*C*) Stroke patients without hand motor deficits also showed a maximum, albeit low lesion overlap at the internal capsule region (n = 5/20). This indicates that the lesion location within the internal capsule is not always associated with impairment of upper limb function. Lesion maps were normalized to an MNI reference brain. Lesion overlap was created using MRIcron (http://www.mccauslandcenter.sc.edu/mricro/mricron/index.html). For individual lesion maps, see Supplementary Figure 1.

Materials and Methods

Sample

The study was approved by the local ethics committee (File No. 11–191). From November 2011 to March 2013, we screened patients from the stroke unit, Department of Neurology, University of Cologne, for study eligibility. Inclusion criteria for stroke patients were as follows: 1) first-ever ischemic stroke as verified by diffusion-weighted imaging (DWI) (Fig. 1; for the location of individual lesions, see Supplementary Fig. 1), 2) cortical and/or subcortical lesions sparing M1, 3) symptom onset <8 days, and 4) age: 30–99 years. Exclusion criteria were as follows: 1) hemorrhagic stroke, 2) contraindications to MRI, 3) previous stroke as detected on FLAIR images, 4) bi-hemispheric stroke lesions, 5) carotid artery stenosis >50% according to the NASCET criteria, 6) intracranial stenosis as tested by transcranial Doppler, 7) cognitive impairment or dementia, 8) impaired consciousness, and 9) other neurological or psychiatric disease. Forty acute right-handed stroke patients either with unilateral motor deficits of the upper limb ($n = 20$) as well as patients without motor deficits ($n = 20$) were finally enrolled into the study (cf. Table 1 for clinical data). Additionally, we recruited 20 right-handed nonstroke patients from the stroke unit who showed no lesions in FLAIR or DWI images (cf. Table 2). Patients gave informed written consent according to the Declaration of Helsinki.

Magnetic Resonance Imaging

All sequences were part of a clinical MRI protocol for stroke diagnostics acquired on a 1.5T scanner (Philips, Guildford, UK). Axial whole-brain resting-state fMRI scans were obtained using a gradient echo planar imaging (EPI) sequence: TR = 2100 ms, TE = 50 ms, FOV = 250 mm, 24 axial slices, voxel size: $3.9 \times 3.9 \times 3.9$ mm³, 183 volumes, ~6 min. Prior to scanning, patients were instructed to rest motionless and awake. The MRI stroke protocol further included DWI, T2-weighted, T2*-weighted, FLAIR, and time-of-flight angiography sequences (see Supplementary material for details).

Table 1
Clinical data of stroke patients

Patient number	Age (years)	Gender (M, male; F, female)	Time after stroke onset (days)	Affected hemisphere	MI (affected hand score)	Mean MI (affected upper limb)	Mean MI (affected lower limb)	Trunk control test	Grip force Index (% affected/ unaffected)	NIHSS (total)	Modified Rankin Scale	Lesion volume (mm³)
Patients with hand motor impairment ($n = 20$)												
Patient 1	91	F	3	R	0	0	9	3	0	21	4	38 1160
Patient 2	86	F	7	L	0	0	0	0	0	15	5	26 706
Patient 3	65	M	1	L	0	0	0	3	0	12	5	4894
Patient 4	78	F	1	L	0	3	12	6	0	11	4	14 388
Patient 5	71	M	2	L	11	13	14	6	0	7	5	891
Patient 6	89	F	1	R	11	13	21	9	0	6	4	1860
Patient 7	64	M	4	L	0	0	0	0	9	7	5	57 122
Patient 8	72	M	4	L	22	27	25	3	13	12	4	57 621
Patient 9	74	F	5	L	22	17	14	15	19	6	4	36 123
Patient 10	60	M	8	L	22	20	13	9	21	9	4	6183
Patient 11	50	F	5	L	22	27	28	25	23	4	3	2892
Patient 12	74	F	4	R	26	29	33	25	31	1	1	7064
Patient 13	69	M	1	L	19	29	33	25	35	3	3	1920
Patient 14	63	M	4	L	26	19	19	19	38	6	4	2363
Patient 15	89	M	2	R	26	22	22	9	42	6	4	1762
Patient 16	72	M	5	L	11	4	0	3	44	12	4	77 709
Patient 17	57	M	4	L	22	29	33	25	50	4	2	4361
Patient 18	84	F	2	L	26	29	33	25	55	3	2	12 346
Patient 19	70	M	5	R	26	24	30	25	56	1	3	2433
Patient 20	64	M	1	L	26	25	33	25	60	5	3	3098
MEAN	72.1		3. 5		15.9	16.5	18.6	13.0	24.8	8	4	35 145
SD	11.4		2.1		10.6	11.4	12.4	10.1	21.7	5	1	84 527
Patients without hand motor impairment ($n = 20$)												
Patient 21	39	M	2	R	33	33	33	25	90	0	0	1222
Patient 22	67	F	4	R	33	31	33	25	90	0	0	7125
Patient 23	85	F	4	L	33	33	33	25	91	1	0	537
Patient 24	81	M	3	L	33	33	33	25	94	1	0	992
Patient 25	69	M	4	L	33	33	33	25	94	3	0	8583
Patient 26	74	M	1	L	33	33	33	25	95	2	0	1151
Patient 27	74	M	3	L	33	33	33	25	99	1	0	1070
Patient 28	60	M	1	R	33	33	33	25	106	3	0	4678
Patient 29	76	M	1	L	33	33	33	25	106	2	0	1306
Patient 30	82	F	5	R	33	33	33	25	107	2	0	1627
Patient 31	69	F	1	L	33	33	33	25	109	1	0	1677
Patient 32	72	F	5	L	33	33	33	25	112	2	0	4776
Patient 33	84	M	2	L	33	33	33	25	116	2	0	2761
Patient 34	43	M	1	L	33	33	33	25	119	2	0	4860
Patient 35	68	M	1	L	33	33	33	25	121	6	0	105 560
Patient 36	81	F	1	L	33	33	33	25	122	2	0	71 226
Patient 37	79	F	8	L	33	33	33	25	122	1	0	749
Patient 38	82	F	1	L	33	30	33	25	132	0	0	3895
Patient 39	75	F	6	L	33	31	30	22	136	1	0	1168
Patient 40	69	F	1	L	33	33	33	25	138	5	0	6642
MEAN	71.5		2.8		33	32.6*	32.9	24.8	111.0	2	0	11 580
SD	12.3		2.1		0	0.9	0.6	0.7	15.1	2	0	26 958

Note: *Note that the MI score for the upper limb was slightly reduced in 3 patients without hand motor impairment as they had difficulties to move the proximal muscles of elbow and shoulder against external resistance despite full grip force and hand motor performance.
MI, Motricity Index; NIHSS, National Institutes of Health Stroke Scale.

Behavioral Tests

We assessed motor function in a brief bedside test at the day of the MRI. Global neurological impairment was rated using the National Institutes of Health Stroke Scale (NIHSS). Motor performance was measured using the Motricity Index (MI) (Demeurisse et al. 1980). The MI is a brief rating scale based on movements of the proximal, middle, and distal joints of arms and legs, which are classified according to whether they can be performed against gravity or even against resistance. Normal motor performance is rated by a maximum score of 33 per item. Additionally, the maximum grip force was assessed for each hand in 3 consecutive trials using a vigorimeter. We computed a grip force index representing the percent grip force of the stroke-affected relative to the unaffected hand (i.e., mean grip force [stroke-affected hand]/mean grip force [unaffected hand] × 100).

Clinical Definition of Motor Impairment Groups

To decode neuroimaging markers of hand motor impairment after stroke based on M1 resting-state connectivity patterns, we defined 2 groups of stroke patients either with hand motor impairment or without hand motor impairment based on the grip force index and the MI score of the stroke-affected hand. Patients without hand motor impairment were defined to have 1) preserved grip strength as indicated by a grip force index of ≥ 90% and 2) the maximum MI hand score of 33 (Table 1). These criteria guaranteed that none of the patients in this group featured significant hand weakness.

In contrast, patients with hand motor deficits were defined to show 1) considerable hand weakness as indicated by a grip force index of ≤2/3 (66%) and 2) an MI score of the stroke-affected hand of ≤26. The grip force criterion ensured that reduced grip strength was indeed caused by stroke as it has been previously shown that differences in handedness may result in reductions of the grip force index of up to 30% (Crosby et al. 1994). The MI criterion implied that hand movements could not be performed against resistance or even gravity. Finally, 40 patients fulfilled the criteria of being assigned to either group. Nonstroke controls showed normal motor performance (grip force ≥ 90%, MI = 33) (Table 2). We compared clinical parameters, age, and gender between groups using ANOVA or chi-squared tests in SPSS21 (IBM, New York).

Resting-State fMRI Analysis

Resting-state fMRI data were analyzed using Statistical Parametric Mapping (SPM8; http://www.fil.ion.ucl.ac.uk/spm/) and Matlab

Table 2
Clinical data of nonstroke neurological patients (control group)

Patient number	age (years)	gender (M, male; F, female)	Mean MI (affected upper limb)	Mean MI (affected lower limb)	Trunk Control Test	Grip force Index (% affected/ unaffected)	Modified Rankin Scale	Clinical diagnosis
Control 1	79	M	33	33	25	90	0	TIA
Control 2	72	F	33	33	25	93	0	Meningitis
Control 3	75	F	33	33	25	94	0	TIA
Control 4	46	F	33	33	25	95	0	AION
Control 5	27	M	33	33	25	96	0	TIA
Control 6	50	M	33	33	25	99	0	TIA
Control 7	56	M	33	33	25	100	0	Peripheral facial nerve palsy
Control 8	74	M	33	33	25	104	0	AION
Control 9	54	M	33	33	25	104	0	Migraine
Control 10	70	M	33	33	25	104	0	TIA
Control 11	72	M	33	33	25	105	0	TIA
Control 12	72	F	33	33	25	105	0	Amaurosis fugax
Control 13	81	F	33	33	25	105	0	TIA
Control 14	57	M	33	33	25	105	0	TIA
Control 15	53	F	33	33	25	105	0	TIA
Control 16	38	M	33	33	25	106	0	TIA
Control 17	81	M	33	33	25	116	0	TIA
Control 18	67	F	33	33	25	124	0	TIA
Control 19	71	F	33	33	25	127	0	TIA
Control 20	92	F	33	33	25	148	0	TIA
MEAN	64.4		33.0	33.0	25.0	106.3	0.0	
SD	16.2		0.0	0.0	0.0	13.6	0.0	

AION, anterior ischemic optic neuropathy; TIA, transitory ischemic attack.

R2012a (The Mathworks, Natick, MA, USA) according to standard preprocessing protocols (Rehme et al. 2013). The first 3 images of the time-series were discarded. The remaining 180 resting-state EPI volumes were spatially realigned to the mean image of the time-series and co-registered with the structural T2-weighted image. Then, all images were spatially normalized to the standard template of the Montreal Neurological Institute (MNI, Canada) using the unified segmentation approach with masked lesions (Ashburner and Friston 2005). Finally, data were smoothed with an isotropic Gaussian kernel of 8 mm. After preprocessing, the effect of known confounds was removed from the time-series. Confound regressors included the mean-centered global, gray matter, white matter, and cerebrospinal fluid signal intensities and their squared values, the 6 head motion parameters from image realignment, their squared values as well as their first-order derivatives (Satterthwaite et al. 2013). Furthermore, the time-series was adjusted for the first 5 components of a principal component analysis (Behzadi et al. 2007; Chai et al. 2012). Data were then band-pass filtered between 0.01 and 0.08 Hz. The majority of the stroke patients had left-hemispheric stroke lesions ($n = 31/40$ patients). Patients with right-hemispheric lesions were equally distributed in the 2 stroke groups ($n = 5$ with hand motor deficits, $n = 4$ without hand motor deficits). Thus, for group comparisons, data of these 9 patients were flipped along the midsagittal plane. Consequently, the left hemisphere corresponded to the ipsilesional hemisphere in all patients. We tested for group differences in head motion parameters from image realignment by comparing the framewise displacement and the root mean squared error (RMSE) (Power et al. 2012). There was no difference between groups neither in the framewise displacement ($F_{2,57} = 0.126$, $P = 0.882$) nor in the RMSE ($F_{2,57} = 0.158$, $P = 0.854$).

Resting-state connectivity maps of ipsilesional M1 were obtained by computing voxelwise whole-brain correlations of time-courses with the ipsilesional M1 seed region, which were transformed into Fisher Z-scores (Biswal et al. 1995). The M1 seed coordinate was defined from a meta-analysis on neural activity for hand motor tasks and was located at the rostral wall of the central sulcus at the "hand knob" area (Rehme et al. 2012). Note that none of the subjects suffered from lesions in M1 as verified by structural scans (DWI, FLAIR, T2).

Multivariate SVM Analysis

SVM Features

We used 1) voxels of individual resting-state connectivity maps representing the functional connectivity between M1 seed region and whole-brain target voxels and 2) voxels of binary DWI lesion maps as input variables (= features) for classification.

To focus on the cortical resting-state motor network and ensure an identical number of voxelwise features per patient, individual resting-state maps were masked by cytoarchitectonic probability maps of frontoparietal sensorimotor areas (Eickhoff et al. 2005) (Brodmann areas 6, 4a/b, 3a/b, 1, 2) using FSLv5.0 (http://fsl.fmrib.ox.ac.uk). Thus, after masking, the resting-state functional connectivity map consisted of 67 957 voxelwise feature variables.

Voxelwise connectivity as a linear parameter was scaled to range between 0 and 1. To increase predictive power and reduce noise, we computed Fisher's criterion score for feature selection (Müller et al. 2004; Feis et al. 2013). This separation index reflects the squared difference between group means in relation to intragroup variance for each feature. In the leave-one-subject-out cross-validation approach described later, feature selection was carried out for each training sample separately. The classification of one left-out subject was based on the features selected in the respective training sample. This procedure guaranteed that the classification of data in the testing step was inherently independent from the selection criteria applied in the training step to prevent "double dipping" (Kriegeskorte et al. 2009). For each training sample, we entered 5% of the most discriminative voxels of the resting-state connectivity maps (i.e., 3398 features per patient) into the SVM algorithm.

To test whether lesion location can be used to classify motor impairment after stroke, one SVM was set up based on the whole-brain DWI lesion maps, which were masked by a summary map of all lesions (178 437 voxelwise features per patient). In this way, noninformative voxels where none of the patients showed a lesion were removed from the analysis. Furthermore, to consider only corticospinal tract (CST) lesions for classification, we masked the lesion maps with a probabilistic map of the CST (Oishi et al. 2010), which yielded 27 437 features per patient.

SVM Classification

We computed 3 different linear two-class SVMs using the Library for SVMs (Chang and Lin 2011) (http://www.csie.ntu.edu.tw/~cjlin/libsvm/) to classify patients according to 1 of 3 groups: stroke patients without hand motor impairment, stroke patients with hand motor deficits, and nonstroke controls.

Each SVM was trained and tested using a nested leave-one-subject-out cross-validation procedure (Fig. 2) (Müller et al. 2004; Dosenbach et al. 2010; Feis et al. 2013). In the outer loop, one subject was

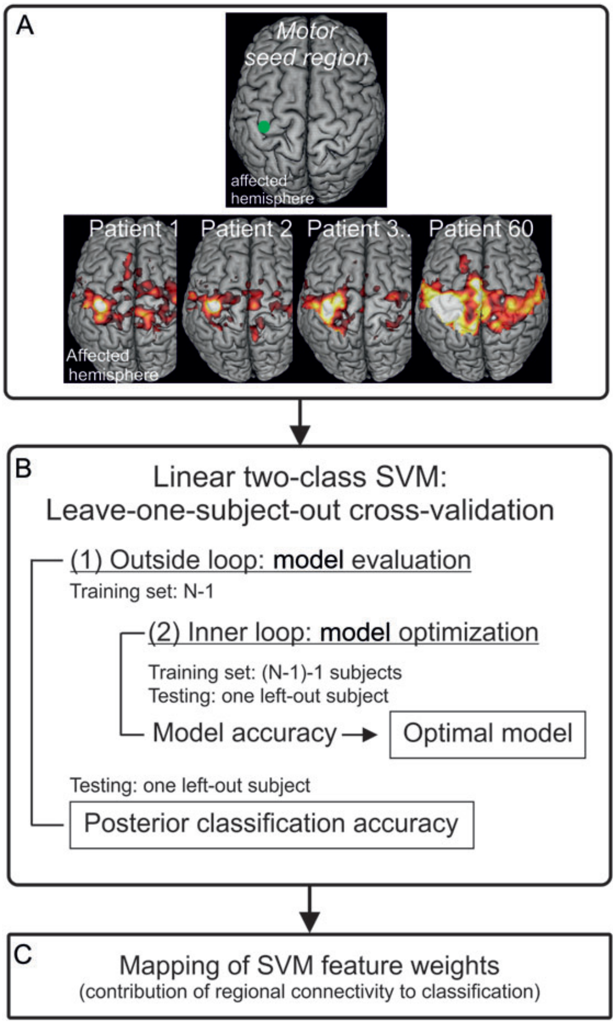

Figure 2. SVM design. (*A*) Preparing feature variables for the SVM analysis. The left panel shows the seed region at the hand knob formation in primary motor cortex (M1) of the ipsilesional (affected) hemisphere, which was used to compute voxelwise correlation maps with every voxel within frontoparietal brain areas (cf. Methods). The right panel shows individual examples of resting-state functional connectivity maps. Each map consisted of 67 957 feature variables. Based on Fisher's criterion (cf. Methods), 5% of the most discriminative voxelwise features (= connectivity values) for each training data set were entered into the SVM analyses. (*B*)Linear two-class SVM with a nested leave-one-subject-out cross-validation procedure. The outside loop was for model evaluation. Here, in a leave-one-subject-out cross-validation procedure, one subject was left out as a test sample and the rest of the sample constituted the training sample (N-1). The inner loop was for model optimization with a second leave-one-subject-out cross-validation procedure based on the training data. The model was optimized using different C-parameters of a linear decision function. The model with the highest accuracy and generalizability of the inner loop was used for classifying the left out, unknown subject of the outer loop. The posterior balanced accuracy was computed across all outer model evaluation loops. (*C*) The SVM weights of the linear separation function were reconstructed for all patients (cf. Methods). These weights show voxelwise connectivity values that contribute to SVM classification.

considered as the test sample and thus set aside whereas all remaining subjects formed the training sample (N-1). Feature selection was repeated for each training sample. Then, the classification model was optimized based on different soft margin constants of the linear separation boundary (i.e., C-parameters ranging from small [C = 0.0001] to large [C = 30]). For this optimization, we used another leave-one-subject-out cross-validation procedure by successively omitting and classifying one subject of the training data. In the outer loop, the model with the highest accuracy and the highest generalizability (i.e., smallest C-parameter) of the inner loop was used to classify the left-out, unknown subject (test sample). The outer loop was repeated for each subject left out and being classified based on the model optimized for the rest of the sample. Thus, training and testing were entirely independent steps (Kriegeskorte et al. 2009). We then computed the posterior balanced accuracy of classifications across all outer loops and reported 95% confidence intervals (CIs) (Brodersen et al. 2010). The significance of this classification was tested using chi-squared tests for equal distributions of correct and incorrect classifications. Finally, we reconstructed the SVM feature weights for the feature selection of each training data set and averaged these weights across all 40 training sets to visualize the voxels that mostly contributed to classification.

Confound Analysis

We carried out SVM control analyses with the same leave-one-subject-out cross-validation approach to test whether group classification may already be explained by a sampling bias (e.g., idiosyncrasies of the study groups). Age and the RMSE of the head motion parameters were included as potential confounds for all 3 groups into the analysis. For stroke patients, we also considered lesion volume and time after stroke onset as potential confounds. All parameters were linearly scaled to range between 0 and 1. We first conducted univariate SVM analyses for each confound, separately, followed by an SVM with all confounds but without neuroimaging data. We then combined the features of interest (i.e., resting-state connectivity and DWI lesion maps) with the different confound variables.

Mass-Univariate GLM Group Analyses

We were interested whether resting-state markers for individual motor impairment revealed by multivariate SVM feature weights were comparable with the results of a conventional group analysis computed within the framework of the GLM. To this end, we used the same connectivity maps as for the SVM analysis consisting of positive correlations between seed voxel time-courses in ipsilesional M1 and whole-brain target voxels, which were transformed into Fisher Z-scores and then masked by frontoparietal sensorimotor areas (Eickhoff et al. 2005). To warrant consistency between multivariate and univariate procedures, we computed separate independent samples t-tests with SPM to obtain T-contrast images for comparisons between controls and stroke patients ($P < 0.05$).

Mass-Univariate Decoding Analysis

To directly compare multivariate SVM classification with univariate decoding, we tested the classification accuracy of individual voxels for the discrimination of the 3 groups. We used the same approach as in the SVM training consisting of a leave-one-subject-out cross-validation procedure with a training sample and one independent test sample. For each voxel of the average SVM weight image, the mean of the average connectivity in each group of the training data set was used as a separation boundary to classify the respective left-out subject. Finally, the classification accuracy for each voxel was averaged across all cross-validation loops.

Expert Rating of DWI Lesions

Additionally, we performed a clinical rating with 9 certified consultant neurologists (Department of Neurology, University of Cologne, Germany; >5 years of clinical experience) using printouts of the axial DWI slices showing the entire extent of the lesion. The raters were asked to indicate whether the respective patient has a hand motor deficit or not. We then computed the posterior accuracy of these clinical ratings (Brodersen et al. 2010).

Comparison of Classification Accuracies

We compared classification accuracies between 1) resting-state connectivity data, 2) DWI lesion maps, and 3) clinical ratings of each of the 9 raters using McNemar's chi-squared test of the null hypothesis that classification is equal across these modalities ($P < 0.05$, one-tailed) (McNemar 1947).

Results

Sample

There was no significant difference in age and gender between groups ($P \geq 0.139$) (Tables 1 and 2; see Supplementary Table 1 for statistical comparisons). Likewise, the two stroke groups did not differ in time after stroke onset or lesion volume ($P \geq 0.242$). The stroke group with hand motor deficits showed a mean grip force index of 24.8% (SD: 21.7%) and a mean MI hand score of 15.9 (10.6). In contrast, stroke patients without hand motor deficits had an MI hand score of 33 and a mean grip force of 111% (15.1%). Hence, patients with motor deficits exhibited significantly worse motor performance than stroke patients with normal hand motor performance and nonstroke controls ($P < 0.001$). There was no difference in motor performance between stroke patients without hand motor deficit and controls ($P > 0.5$).

Resting-State Functional Connectivity

Univariate Group Analyses (GLM)

SPM-T-contrast images for the comparison of stroke patients with hand motor deficits and nonstroke controls showed that nonstroke controls featured greater interhemispheric resting-state connectivity between ipsilesional (left) M1 and contralesional sensorimotor areas including contralesional M1, primary sensory cortex (S1), superior parietal lobe (SPL) as well as contralesional dorsal and ventral premotor cortex (PMC) ($P < 0.05$; Fig. 3*A*, blue color scale). This means that patients with hand motor deficits showed reduced connectivity between these areas. In contrast, stroke patients with hand motor deficits as compared with nonstroke controls featured greater resting-state connectivity between ipsilesional M1 and supplementary motor area (SMA), as well as ventral and dorsal PMC, particularly in the ipsilesional hemisphere (Fig. 3*A*, red color scale). The SPM-T-contrasts for the comparison between stroke patients with and without hand motor impairment revealed similar results (Fig. 3*B*). Again, stroke patients with hand motor deficits were characterized by reduced interhemispheric resting-state connectivity between ipsilesional M1 and contralesional sensorimotor areas (Fig. 3*B*, blue color scale) but showed enhanced connectivity between ipsilesional M1 and ipsilesional as well as contralesional premotor areas including SMA and ventral PMC (Fig. 3*B*, red color scale).

Multivariate SVM Classification: Stroke Patients with Motor Impairment versus Nonstroke Controls

The SVM classifying stroke patients with hand motor deficits and controls showed that resting-state connectivity of ipsilesional (left) M1 yielded a posterior classification accuracy of 82.6% ($P < 0.001$, CI = 66.9–90%) (Fig. 4*A*). We observed a similar accuracy when patients with right-hemispheric lesions who had been flipped for group comparisons were omitted

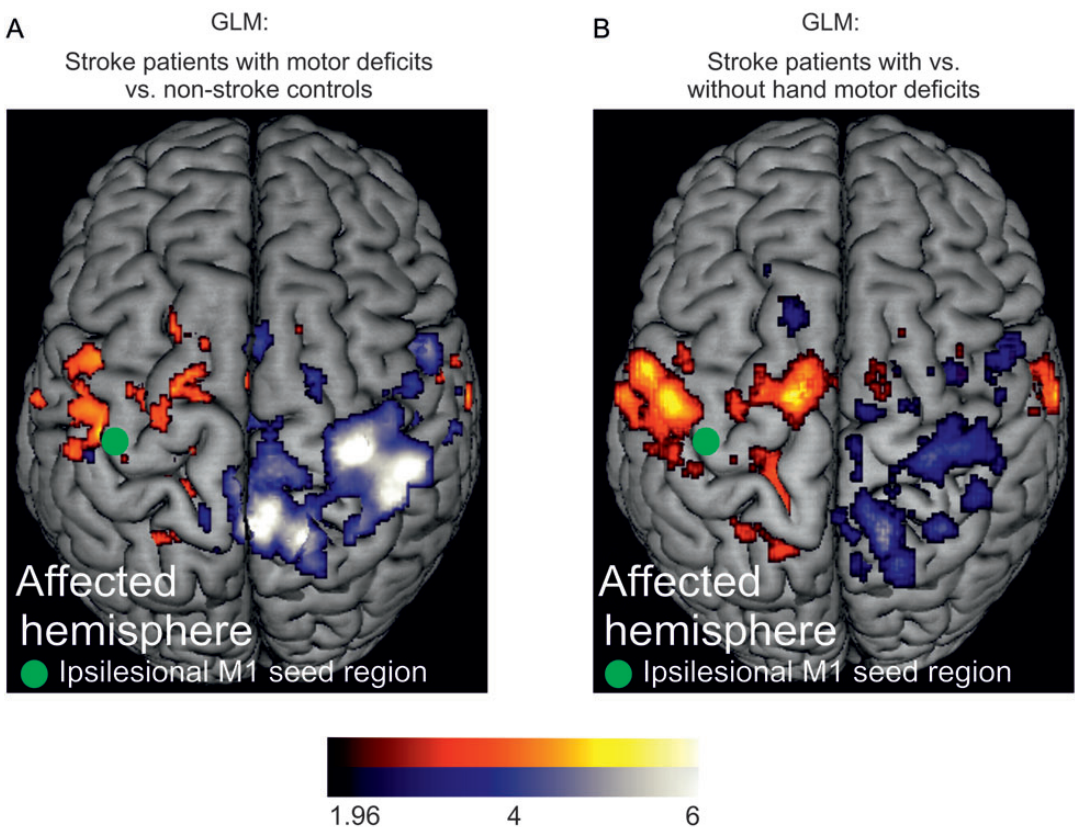

Figure 3. GLM results. (*A*) Group differences (independent samples *t*-test) between stroke patients with hand motor impairment and nonstroke control subjects. Blue: Areas of voxelwise resting-state connectivity for the SPM-T-contrast "controls > patients." Red: Areas of voxelwise resting-state connectivity for the SPM-T-contrast "patients > controls." (*B*) Group differences between stroke patients with and without hand motor impairment. Blue: Areas of voxelwise resting-state connectivity for the SPM-T-contrast "patients without impairment > patients with hand motor impairment." Red: Areas of voxelwise resting-state connectivity for the SPM-T-contrast "patients with hand motor impairment > patients without hand motor impairment." The green dot indicates the seed voxel coordinate in ipsilesional M1 (-38,-24,58). The color bar indicates the respective *t*-value ($P < 0.05$ uncorrected).

(i.e., 79.6%, $P < 0.001$, CI = 62.6–88.3%). The sensitivity to correctly identify stroke patients with hand motor impairment was 80%. The specificity to identify nonstroke controls was 85%. The mean weight image across all training samples—which represents the regional contribution of voxelwise connectivity to classification—corresponded to the direction and spatial distribution of univariate group differences in the conventional GLM analysis (Fig. 3A). Accordingly, controls were characterized by stronger interhemispheric connectivity between ipsilesional M1 and contralesional sensorimotor areas including M1, S1, and SPL (Fig. 4A). In contrast, enhanced connectivity between ipsilesional M1 and ipsilesional ventral and dorsal PMC, SMA, and contralesional medial S1 contributed to the classification of stroke patients with hand motor impairment. In contrast, the SVM for classifying stroke patients without hand motor impairment and nonstroke controls showed a posterior classification accuracy of 58.5%, which was almost at chance level ($P = 0.155$, CI = 42.7–71.9%). Thus, based on M1 resting-state connectivity, stroke patients without motor impairment could not be distinguished from controls.

Multivariate SVM Classification of Motor Impairment in Stroke Patients

In the next step, we tested whether SVM can be used to differentiate between the 2 stroke groups. Here, resting-state connectivity of ipsilesional M1 correctly classified unseen stroke patients as either with or without hand motor deficit with a posterior accuracy of 87.6% ($P < 0.001$, CI = 72.4–93.2%) (sensitivity: 90%, specificity: 85%). A similar weight pattern as described earlier for classifying nonstroke controls versus patients with hand motor deficits separated the two groups (Fig. 4B). These weights were again similar to the respective univariate group comparison (Fig. 3B). Accordingly, patients with hand motor deficits were characterized by reduced interhemispheric connectivity of ipsilesional M1 with contralesional sensorimotor areas. In contrast, higher resting-state connectivity between ipsilesional M1 and contralesional ventral PMC and ipsilesional premotor areas (i.e., dorsal and ventral PMC, SMA) discriminated stroke patients with impaired hand function compared with stroke patients without hand motor impairment.

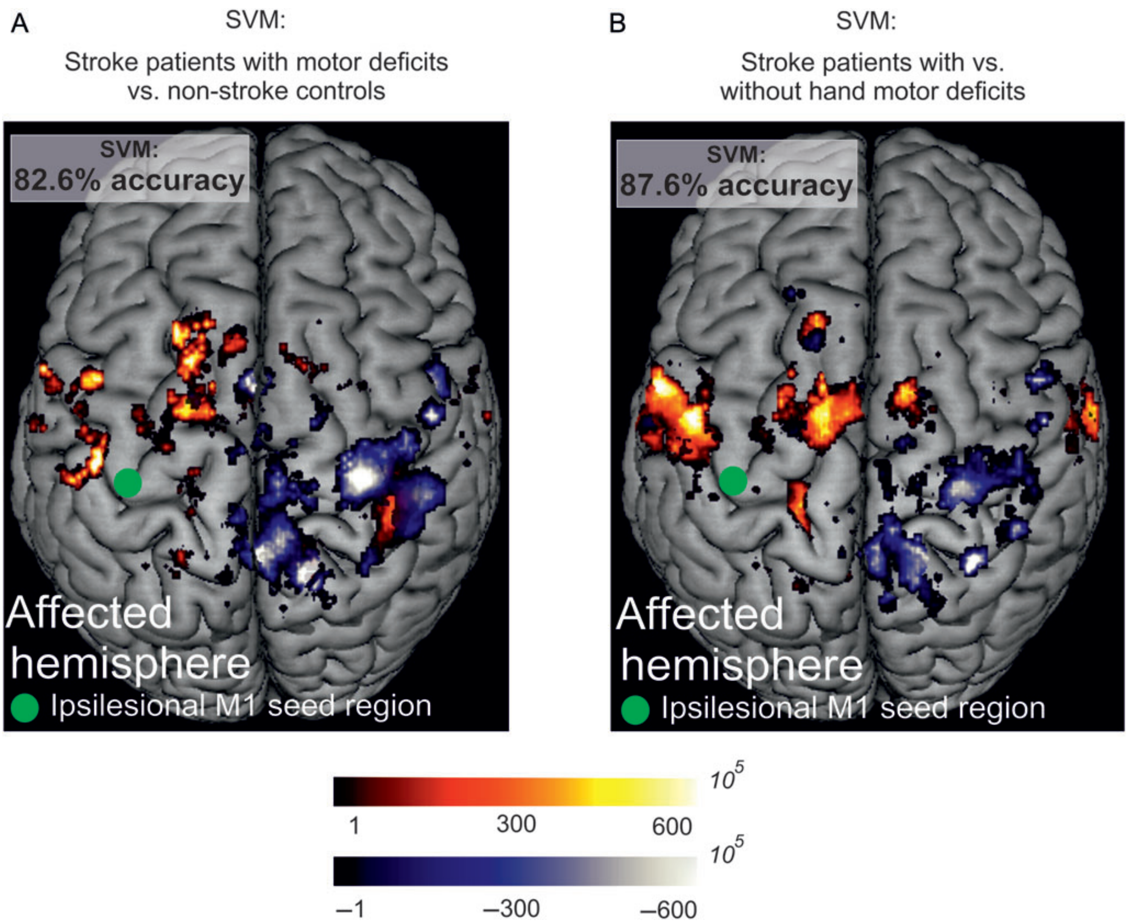

Figure 4. Multivariate SVM classification. (*A*) Results in stroke patients with hand motor impairment and nonstroke controls. Resting-state functional connectivity of ipsilesional M1 provided 82.6% mean accuracy for the classification of unknown patients. The SVM weight image shows the regional contribution of voxelwise resting-state connectivity to the classification of stroke patients with hand motor deficits and nonstroke controls. (*B*) SVM results in stroke patients. Resting-state functional connectivity of ipsilesional M1 provided 87.6% mean accuracy for the classification of stroke patients into hand motor impairment groups. Blue: Areas of voxelwise resting-state connectivity, which contribute to the classification of nonstroke controls (Fig. 4A) or stroke patients without hand motor deficit (Fig. 4B) (i.e., stroke patients with hand motor impairment were characterized by reduced connectivity with these areas). Red: Areas of voxelwise resting-state connectivity, which contribute to the classification of stroke patients with hand motor impairment. The scaling of the weights reflects the relative contribution of voxelwise resting-state connectivity with ipsilesional M1 to group classification. The green dot indicates the seed voxel coordinate in ipsilesional M1 (-38,-24,58).

Mass-Univariate Group Classification

The results of the mass-univariate decoding analyses, using the mean of the average voxel connectivity in each group in each training sample as a boundary to classify the respective left-out subject in a cross-validation approach, showed that more than half of the voxels provided classification accuracies of >50% (Supplementary Fig. 2). However, for the discrimination of stroke patients with hand motor deficits and controls, only 0.2% of the voxels were equal to or better than the classification accuracy of the multivariate SVM classifier of 82.6%. Furthermore, the classification accuracy of 87.6% for separating stroke patients with or without hand motor deficits was only reached by one single voxel in the univariate analysis (i.e., 0.01%). This small proportion was clearly below a 5%-threshold of all voxels. Thus, multivariate decoding seems to outperform univariate decoding in classifying individual patients.

DWI Lesions

The SVM trained with the whole-brain DWI lesion maps considering white matter, cortex, and basal ganglia classified stroke patients with or without hand motor impairment with a posterior accuracy of 67.9% ($P = 0.021$, CI = 50.6–79%). When considering DWI lesions along the CST using probabilistic maps (Oishi et al. 2010), the posterior classification accuracy was 73.8% ($P = 0.003$, CI = 56.4–83.1%). However, the sensitivity to identify patients with motor deficits was low (i.e., 45–50%), whereas the specificity to classify patients without motor deficits was ≥90% (see Supplementary Fig. 3 for the SVM weights). Together, classifications based on DWI lesions tended to be lower than the classification accuracy of resting-state connectivity ($\text{chi}^2(1) = 3.27$, $P = 0.07$).

We further tested how stroke-experienced consultant neurologists ($n = 9$; Department of Neurology, University of Cologne, Germany) classified motor function based on DWI. The posterior accuracy of the raters was 71% ($P < 0.001$, CI = 66–75.3%) (Supplementary Table 2). The SVM for M1 resting-state connectivity classified patients significantly more accurate than 6 out of 9 raters ($P < 0.03$). In contrast, one rater classified patients significantly better than the SVM for DWI lesions, whereas the classifications of the rest of the raters were equal to the SVM results for DWI lesions.

Confound Analysis

We carried out separate and joint SVM control analyses for potential confounds including age, RMSE of head motion parameters, lesion volume, and time after stroke onset. None of these confounds provided a significant group classification (maximum accuracy: 60.1%, $P = 0.106$). Furthermore, combined SVM analyses of confound variables and resting-state connectivity or DWI lesion maps of the CST did not exceed the classification accuracy of each of these feature maps alone (see Supplementary Table 3 for details).

Discussion

This study provides evidence that individual resting-state fMRI scans can be used to decode individual hand motor impairment based on multivariate SVM pattern classification. As expected, conventional univariate analyses of resting-state data revealed a similar pattern of differences between groups as identified by multivariate SVM weights for individual classification. However, only the multivariate SVM analysis approach allowed a significant classification of individual patients with respect to motor impairment. Importantly, motor performance was more accurately classified by M1 resting-state connectivity than by lesion location or by expert rating.

Markers of Motor Impairment after Stroke

SVM classifications are always driven by all features of a given weight vector (Naselaris et al. 2011; Haufe et al. 2014). Here, high weights may reflect both "true" neurophysiological signal and noise. That is, to maximize separation, an optimal classifier may require nonzero weights on features containing the signal of interest as well as on features containing additional noise. In this way, the classifier accounts for the entire structure of the data and provides a more accurate classification. Accordingly, the decoding approach usually does not allow drawing conclusions such that one connection reflects a marker of a clinical parameter. In contrast, the parameters of a forward model, for example a GLM analysis, are physiologically interpretable (Haufe et al. 2014). Therefore, when combined with a forward model approach, SVM weights may be interpreted in terms of their neurophysiological meaning. Figures 3 and 4 show that positive and negative SVM weights spatially correspond to the direction of group differences between patients and controls in the GLM analysis. This correspondence between the backward (SVM) and forward (GLM) model therefore suggests that resting-state connectivity between ipsilesional M1 and these areas significantly contributes to the characterization of impaired hand motor function after stroke.

Accordingly, the SVM classified stroke patients with hand motor deficits based on reduced interhemispheric resting-state connectivity between ipsilesional and contralesional motor areas. This finding was reproduced by contrasting patients with hand motor deficits with independent samples of non-stroke controls and stroke patients with normal hand motor performance (Fig. 4). Our results thus corroborate findings of disturbed interhemispheric connectivity between sensorimotor areas in groups of stroke patients with motor deficits as reported in previous fMRI group studies (Carter et al. 2010, 2012; Wang et al. 2010; Park et al. 2011; Golestani et al. 2013).

Changes in interhemispheric resting-state connectivity may play a key role in early cortical reorganization (Carmichael 2006). Intracranial recordings in humans and animals showed that resting-state connectivity reflects spontaneous oscillations of synchronous neuronal activity (He et al. 2008; Nir et al. 2008; van Meer et al. 2012). There seems to be a close relationship between alterations in synchronous activity remote from the lesion and induction of axonal sprouting in the first few days after stroke (Carmichael and Chesselet 2002). Thus, reduced interhemispheric resting-state connectivity at the acute stage may represent an early imaging marker of neural repair processes after stroke. This conclusion is supported by human fMRI studies probing the motor execution system after stroke by means of motor activation tasks and connectivity analyses (Rehme et al. 2012; Grefkes and Fink 2014). These studies frequently reported enhanced neural activity in contralesional M1 during movements of the stroke-affected hand. In the first few days after stroke, contralesional M1 has been shown to exert a positive influence onto ipsilesional M1 activity, which may support early motor recovery (Rehme, Eickhoff, Wang et al. 2011). Over the ensuing weeks and months, this positive influence disappears or may even turn into maladaptive inhibition in some patients (Grefkes et al. 2008; Rehme, Eickhoff, Wang et al. 2011). Although task-based and resting-state fMRI reflect distinct underlying neural processes (Rehme et al. 2013), findings from fMRI motor activation studies emphasize the role of contralesional M1 as a brain region involved into early motor reorganization that corresponds to the present resting-state findings.

A new finding of the present study is that patients with hand motor deficits were also characterized by enhanced resting-state connectivity between ipsilesional M1 and secondary motor areas in frontoparietal cortex including PMC, SMA, and S1, particularly in the ipsilesional hemisphere. The SVM results show that this increase in connectivity is essential for the individual classification of motor impairment. Findings from previous task-based fMRI studies suggest an important role of premotor areas in post-stroke recovery (Johansen-Berg et al. 2002; Rehme, Fink et al. 2011). These studies demonstrated that an increase of activity in premotor areas during movements of the stroke-affected hand predicts greater motor recovery after stroke. Furthermore, effective connectivity data revealed that positive influences between premotor areas, particularly SMA, and ipsilesional M1 correlate with motor recovery and recovered motor function (Grefkes et al. 2008; Wang et al. 2011; Rehme, Eickhoff, Wang et al. 2011). Likewise, Park and colleagues showed that higher resting-state connectivity between ipsilesional M1 and contralesional SMA at the acute stage predicts motor performance at the chronic stage after stroke (Park et al. 2011). Thus, as premotor neurons are engaged in motor preparation and higher-order movement control (Dum and Strick 2002), increased connectivity between M1 and premotor areas may reflect a neural disposition facilitating early cortical reorganization. Indeed, in chronic stroke patients, transcranial magnetic stimulation studies have shown that disruption of both ipsilesional and contralesional dorsal PMC activity can deteriorate recovered motor function as assessed with reaction time or sequential finger movement tasks (Fridman et al. 2004; Lotze et al. 2006). In the present study, we used a rather simple motor assessment that could be easily performed at the bedside, even with patients suffering from severe hemiplegia. It remains to be elucidated whether similar weight distributions would be observed when using more complex motor tasks to quantify the hand motor deficit.

The Diagnostic Use of SVM and fMRI

Ipsilesional M1 resting-state connectivity provided a high sensitivity of ≥80% to identify unknown patients with hand motor deficits when comparing them with stroke patients with normal hand motor performance or nonstroke controls. In contrast, the multivariate SVM classifier did not discriminate stroke patients with normal motor performance and controls. Our data, therefore, suggest that resting-state motor networks are not altered after stroke per se but rather allow specific inference about motor impairment. The direct comparison with mass-univariate decoding analyses showed that most of the individual voxels had some power to discriminate previously unseen patients. However, the accuracy of multivariate SVM classifiers was only exceeded by 0.2% of the voxels. Our findings, therefore, suggest that the combined information from multiple voxels is more powerful than single voxels, which may rather reflect random results. Thus, this finding strengthens the importance of carrying out multivariate rather than univariate decoding analyses. Multivariate machine learning techniques have been successfully applied to resting-state fMRI networks in other clinical populations (Shen et al. 2010; Richiardi et al. 2012; Wee et al. 2012; Zeng et al. 2012). These studies reported accuracies of 70–96%, which are consistent with the ones we observed in our sample. Thus, although resting-state fMRI is measured in a task-free setting, it allows classifying clinical populations at the single subject level.

With respect to neuroimaging markers of functional impairment after stroke, Saur and colleagues showed that SVM can predict good versus poor recovery from aphasia with 86% accuracy based on early fMRI activation during a language task in combination with age and the initial language test score (Saur et al. 2010). In contrast to this study, we used resting-state fMRI, which is particularly useful in clinical routine assessment of acute, severely disabled patients because it yields robust signals after only 5–6 min and requires no task-related behavior (Friston 1994; Carter et al. 2010; Van Dijk et al. 2010; Wang et al. 2010).

Furthermore, our findings are well in line with previous conventional univariate resting-state group studies in stroke patients, which demonstrated that disturbances in connectivity are specific to the functional system that has been damaged. For example, stroke patients with motor deficits, aphasia, or visual neglect show disturbed resting-state connectivity in the corresponding motor, language, or attention resting-state networks (He et al. 2007; Warren et al. 2009; Carter et al. 2010). Importantly, our findings extend the results of previous univariate encoding analyses performed at the group level by showing that multivariate decoding approaches for resting-state fMRI data enable classification at the level of an individual patient. Given that a single resting-state fMRI scan allows simultaneous assessment of different resting-state networks, SVMs for resting-state data might be suited to classify patients with aphasia or attention deficits (He et al. 2007; Warren et al. 2009; Carter et al. 2010) but also to ultimately classify the global neurological deficit and potential for recovery.

Acute Ischemic Lesion

The SVM accuracy for the classification of hand motor deficits based on structural lesions was 73.8%. However, the SVM provided a poor sensitivity of 50% to identify patients with hand motor deficits. Likewise, we observed a similar degree of classification accuracy in the ratings of experienced consultant neurologists, which suggests that expert knowledge of functional brain anatomy is not sufficient to ensure correct classifications.

Hence, stroke lesions provide a less reliable classification of motor deficits at the level of individual patients compared with resting-state connectivity. At first, this finding seems to be at odds with previous diffusion tensor imaging (DTI) studies showing that greater motor impairment was associated with greater disruptions of CST fibers, particularly of those extending from ipsilesional M1 (Stinear et al. 2007; Lindenberg et al. 2012; Wang et al. 2012). However, in contrast to these correlation analyses, individual predictions made by SVM classification are based on a multivariate approach. Here, classifier rules are learned based on a valid training step. Thus, the low sensitivity (50%) revealed by the SVM analysis most likely results from the heterogeneity of lesions that may cause motor deficits in our sample (Fig. 1; Supplementary Fig. 1). This heterogeneity particularly constrains the SVM performance, which depends on the consistency of lesion locations within one group. In contrast to our findings, previous clinical machine learning studies using structural MRI data yielded higher accuracies of 83–96%, particularly for classifying patients with dementia compared with healthy subjects (Klöppel et al. 2008; Gerardin et al. 2009). These differences in classification accuracies may result from different structural data (i.e., DTI, high-resolution T1-weighted images). However, in stroke, even small lesions may cause severe deficits, a phenomenon that contrasts with findings in neurodegenerative disease, which usually affects large parts of the brain (Orrù et al. 2012). Thus, functional neuroimaging markers seem to be superior when classifying functional deficits resulting from confined and heterogeneous lesions, as often encountered after stroke.

Conclusion

We here show that the combination of resting-state fMRI and multivariate machine learning tools constitutes a sensitive technique to infer neurological impairment at the level of single patients. All data were acquired during a routine imaging session, which highlights the clinical practicability of our approach with acute, severely disabled patients (Friston 1994; Carter et al. 2010; Van Dijk et al. 2010; Wang et al. 2010). It should be tested in the future whether this approach offers potential for providing noninvasive diagnostic markers to predict the neurological outcome and to optimize rehabilitation after stroke.

Supplementary Material

Supplementary material can be found at: http://www.cercor.oxfordjournals.org/

Funding

C.G. is supported by the German Research Foundation (DFG GR 3285/2-1; GR 3285/4-1). G.R.F. gratefully acknowledges support by the Marga and Walter Boll Stiftung.

Notes

We thank the MR staff from the Department of Neuroradiology, University of Cologne, for their support in assessing resting-state fMRI scans in acute stroke patients during clinical routine. We further thank Martha Kutscha for her help in data management. *Conflict of Interest*: None declared.

References

Ashburner J, Friston KJ. 2005. Unified segmentation. Neuroimage. 26:839–851.

Behzadi Y, Restom K, Liau J, Liu TT. 2007. A component based noise correction method (CompCor) for BOLD and perfusion based fMRI. Neuroimage. 37:90–101.

Biswal B, Yetkin FZ, Haughton VM, Hyde JS. 1995. Functional connectivity in the motor cortex of resting human brain using echo-planar MRI. Magn Reson Med. 34:537–541.

Brodersen KH, Ong CS, Stephan KE, Buhmann JM. 2010. The balanced accuracy and its posterior distribution. Proceedings of the 20th International Conference on Pattern Recognition. 3121–3124.

Carmichael ST. 2006. Cellular and molecular mechanisms of neural repair after stroke: making waves. Ann Neurol. 59:735–742.

Carmichael ST, Chesselet MF. 2002. Synchronous neuronal activity is a signal for axonal sprouting after cortical lesions in the adult. J Neurosci. 22:6062–6070.

Carter AR, Astafiev SV, Lang CE, Connor LT, Rengachary J, Strube MJ, Pope DL, Shulman GL, Corbetta M. 2010. Resting interhemispheric functional magnetic resonance imaging connectivity predicts performance after stroke. Ann Neurol. 67:365–375.

Carter AR, Patel KR, Astafiev SV, Snyder AZ, Rengachary J, Strube MJ, Pope A, Shimony JS, Lang CE, Shulman GL et al. 2012. Upstream dysfunction of somatomotor functional connectivity after corticospinal damage in stroke. Neurorehabil Neural Repair. 26:7–19.

Chai XJ, Castanon AN, Ongur D, Whitfield-Gabrieli S. 2012. Anticorrelations in resting state networks without global signal regression. Neuroimage. 59:1420–1428.

Chang CC, Lin CJ. 2011. LIBSVM: A library for support vector machines. ACM Trans Intell Syst Technol. 27:1–39.

Chollet F, DiPiero V, Wise RJ, Brooks DJ, Dolan RJ, Frackowiak RS. 1991. The functional anatomy of motor recovery after stroke in humans: a study with positron emission tomography. Ann Neurol. 29:63–71.

Cortes C, Vapnik V. 1995. Support-vector networks. Machine Learn. 20:273–297.

Crosby CA, Wehbe MA, Mawr B. 1994. Hand strength: normative values. J Hand Surg Am. 19:665–670.

Demeurisse G, Demol O, Robaye E. 1980. Motor evaluation in vascular hemiplegia. Eur Neurol. 19:382–389.

Dosenbach NU, Nardos B, Cohen AL, Fair DA, Power JD, Church JA, Nelson SM, Wig GS, Vogel AC, Lessov-Schlaggar CN et al. 2010. Prediction of individual brain maturity using fMRI. Science. 329:1358–1361.

Dum RP, Strick PL. 2002. Motor areas in the frontal lobe of the primate. Physiol Behav. 77:677–682.

Eickhoff SB, Stephan KE, Mohlberg H, Grefkes C, Fink GR, Amunts K, Zilles K. 2005. A new SPM toolbox for combining probabilistic cytoarchitectonic maps and functional imaging data. Neuroimage. 25:1325–1335.

Feis DL, Brodersen KH, von Cramon DY, Luders E, Tittgemeyer M. 2013. Decoding gender dimorphism of the human brain using multimodal anatomical and diffusion MRI data. Neuroimage. 70:250–257.

Fridman EA, Hanakawa T, Chung M, Hummel F, Leiguarda RC, Cohen LG. 2004. Reorganization of the human ipsilesional premotor cortex after stroke. Brain. 127:747–758.

Friston KJ. 1994. Functional and effective connectivity in neuroimaging: a synthesis. Hum Brain Mapp. 2:56–78.

Friston KJ, Holmes AP, Poline JB, Grasby PJ, Williams SC, Frackowiak RS, Turner R. 1995. Analysis of fMRI time-series revisited. Neuroimage. 2:45–53.

Gerardin E, Chetelat G, Chupin M, Cuingnet R, Desgranges B, Kim HS, Niethammer M, Dubois B, Lehericy S, Garnero L et al. 2009. Multidimensional classification of hippocampal shape features discriminates Alzheimer's disease and mild cognitive impairment from normal aging. Neuroimage. 47:1476–1486.

Go AS, Mozaffarian D, Roger VL, Benjamin EJ, Berry JD, Borden WB, Bravata DM, Dai S, Ford ES, Fox CS et al. 2013. Heart disease and stroke statistics--2013 update: a report from the American Heart Association. Circulation. 127:e6–e245.

Golestani AM, Tymchuk S, Demchuk A, Goodyear BG. 2013. Longitudinal evaluation of resting-state FMRI after acute stroke with hemiparesis. Neurorehabil Neural Repair. 27:153–163.

Grefkes C, Fink GR. 2014. Connectivity-based approaches in stroke and recovery of function. Lancet Neurol. 13:206–216.

Grefkes C, Nowak DA, Eickhoff SB, Dafotakis M, Kust J, Karbe H, Fink GR. 2008. Cortical connectivity after subcortical stroke assessed with functional magnetic resonance imaging. Ann Neurol. 63:236–246.

Haufe S, Meinecke F, Gorgen K, Dahne S, Haynes JD, Blankertz B, Biessmann F. 2014. On the interpretation of weight vectors of linear models in multivariate neuroimaging. Neuroimage. 87:96–110.

He BJ, Snyder AZ, Vincent JL, Epstein A, Shulman GL, Corbetta M. 2007. Breakdown of functional connectivity in frontoparietal networks underlies behavioral deficits in spatial neglect. Neuron. 53:905–918.

He BJ, Snyder AZ, Zempel JM, Smyth MD, Raichle ME. 2008. Electrophysiological correlates of the brain's intrinsic large-scale functional architecture. Proc Natl Acad Sci USA. 105:16039–16044.

Johansen-Berg H, Dawes H, Guy C, Smith SM, Wade DT, Matthews PM. 2002. Correlation between motor improvements and altered fMRI activity after rehabilitative therapy. Brain. 125:2731–2742.

Kay KN, Gallant JL. 2009. I can see what you see. Nat Neurosci. 12:245.

Kay KN, Naselaris T, Prenger RJ, Gallant JL. 2008. Identifying natural images from human brain activity. Nature. 452:352–355.

Klöppel S, Stonnington CM, Chu C, Draganski B, Scahill RI, Rohrer JD, Fox NC, Jack CR Jr, Ashburner J, Frackowiak RS. 2008. Automatic classification of MR scans in Alzheimer's disease. Brain. 131:681–689.

Kriegeskorte N. 2011. Pattern-information analysis: from stimulus decoding to computational-model testing. Neuroimage. 56:411–421.

Kriegeskorte N, Simmons WK, Bellgowan PS, Baker CI. 2009. Circular analysis in systems neuroscience: the dangers of double dipping. Nat Neurosci. 12:535–540.

Lemm S, Blankertz B, Dickhaus T, Muller KR. 2011. Introduction to machine learning for brain imaging. Neuroimage. 56:387–399.

Lindenberg R, Zhu LL, Ruber T, Schlaug G. 2012. Predicting functional motor potential in chronic stroke patients using diffusion tensor imaging. Hum Brain Mapp. 33:1040–1051.

Lotze M, Markert J, Sauseng P, Hoppe J, Plewnia C, Gerloff C. 2006. The role of multiple contralesional motor areas for complex hand movements after internal capsular lesion. J Neurosci. 26:6096–6102.

McNemar Q. 1947. Note on the sampling error of the difference between correlated proportions or percentages. Psychometrika. 12:153–157.

Müller K-R, Krauledat M, Dornhege G, Curio G, Blankertz B. 2004. Machine learning techniques for brain-computer interfaces. Biomed Eng. 49:11–22.

Naselaris T, Kay KN, Nishimoto S, Gallant JL. 2011. Encoding and decoding in fMRI. Neuroimage. 56:400–410.

Nir Y, Mukamel R, Dinstein I, Privman E, Harel M, Fisch L, Gelbard-Sagiv H, Kipervasser S, Andelman F, Neufeld MY et al. 2008. Interhemispheric correlations of slow spontaneous neuronal fluctuations revealed in human sensory cortex. Nat Neurosci. 11:1100–1108.

Oishi K, Faria AV, van Zijl PCM, Mori S. 2010. MRI atlas of Human White Matter. Amsterdam: Elsevier.

Orrù G, Pettersson-Yeo W, Marquand AF, Sartori G, Mechelli A. 2012. Using support vector machine to identify imaging biomarkers of neurological and psychiatric disease: a critical review. Neurosci Biobehav Rev. 36:1140–1152.

Park CH, Chang WH, Ohn SH, Kim ST, Bang OY, Pascual-Leone A, Kim YH. 2011. Longitudinal changes of resting-state functional connectivity during motor recovery after stroke. Stroke. 42:1357–1362.

Pereira F, Mitchell T, Botvinick M. 2009. Machine learning classifiers and fMRI: a tutorial overview. Neuroimage. 45:S199–S209.

Power JD, Barnes KA, Snyder AZ, Schlaggar BL, Petersen SE. 2012. Spurious but systematic correlations in functional connectivity MRI networks arise from subject motion. Neuroimage. 59:2142–2154.

Rehme AK, Eickhoff SB, Grefkes C. 2013. State-dependent differences between functional and effective connectivity of the human cortical motor system. Neuroimage. 67:237–246.

Rehme AK, Eickhoff SB, Rottschy C, Fink GR, Grefkes C. 2012. Activation likelihood estimation meta-analysis of motor-related neural activity after stroke. Neuroimage. 59:2771–2782.

Rehme AK, Eickhoff SB, Wang LE, Fink GR, Grefkes C. 2011. Dynamic causal modeling of cortical activity from the acute to the chronic stage after stroke. Neuroimage. 55:1147–1158.

Rehme AK, Fink GR, von Cramon DY, Grefkes C. 2011. The role of the contralesional motor cortex for motor recovery in the early days after stroke assessed with longitudinal FMRI. Cereb Cortex. 21:756–768.

Rehme AK, Grefkes C. 2013. Cerebral network disorders after stroke: evidence from imaging-based connectivity analyses of active and resting brain states in humans. J Physiol. 591:17–31.

Richiardi J, Gschwind M, Simioni S, Annoni JM, Greco B, Hagmann P, Schluep M, Vuilleumier P, Van DV. 2012. Classifying minimally disabled multiple sclerosis patients from resting state functional connectivity. Neuroimage. 62:2021–2033.

Satterthwaite TD, Elliott MA, Gerraty RT, Ruparel K, Loughead J, Calkins ME, Eickhoff SB, Hakonarson H, Gur RC, Gur RE et al. 2013. An improved framework for confound regression and filtering for control of motion artifact in the preprocessing of resting-state functional connectivity data. Neuroimage. 64:240–256.

Saur D, Ronneberger O, Kummerer D, Mader I, Weiller C, Kloppel S. 2010. Early functional magnetic resonance imaging activations predict language outcome after stroke. Brain. 133:1252–1264.

Shen H, Wang L, Liu Y, Hu D. 2010. Discriminative analysis of resting-state functional connectivity patterns of schizophrenia using low dimensional embedding of fMRI. Neuroimage. 49:3110–3121.

Stinear CM, Barber PA, Smale PR, Coxon JP, Fleming MK, Byblow WD. 2007. Functional potential in chronic stroke patients depends on corticospinal tract integrity. Brain. 130:170–180.

Van Dijk KR, Hedden T, Venkataraman A, Evans KC, Lazar SW, Buckner RL. 2010. Intrinsic functional connectivity as a tool for human connectomics: theory, properties, and optimization. J Neurophysiol. 103:297–321.

van Meer MP, Otte WM, van der Marel K, Nijboer CH, Kavelaars A, van der Sprenkel JW, Viergever MA, Dijkhuizen RM. 2012. Extent of bilateral neuronal network reorganization and functional recovery in relation to stroke severity. J Neurosci. 32:4495–4507.

Wang L, Yu C, Chen H, Qin W, He Y, Fan F, Zhang Y, Wang M, Li K, Zang Y et al. 2010. Dynamic functional reorganization of the motor execution network after stroke. Brain. 133:1224–1238.

Wang LE, Fink GR, Diekhoff S, Rehme AK, Eickhoff SB, Grefkes C. 2011. Noradrenergic enhancement improves motor network connectivity in stroke patients. Ann Neurol. 69:375–388.

Wang LE, Tittgemeyer M, Imperati D, Diekhoff S, Ameli M, Fink GR, Grefkes C. 2012. Degeneration of corpus callosum and recovery of motor function after stroke: a multimodal magnetic resonance imaging study. Hum Brain Mapp. 33:2941–2956.

Ward NS, Brown MM, Thompson AJ, Frackowiak RS. 2003. Neural correlates of motor recovery after stroke: a longitudinal fMRI study. Brain. 126:2476–2496.

Ward NS, Newton JM, Swayne OB, Lee L, Thompson AJ, Greenwood RJ, Rothwell JC, Frackowiak RS. 2006. Motor system activation after subcortical stroke depends on corticospinal system integrity. Brain. 129:809–819.

Warren JE, Crinion JT, Lambon Ralph MA, Wise RJ. 2009. Anterior temporal lobe connectivity correlates with functional outcome after aphasic stroke. Brain. 132:3428–3442.

Wee CY, Yap PT, Zhang D, Denny K, Browndyke JN, Potter GG, Welsh-Bohmer KA, Wang L, Shen D. 2012. Identification of MCI individuals using structural and functional connectivity networks. Neuroimage. 59:2045–2056.

World Health Organization. 2004. The Atlas of Heart Disease and Stroke.

Zeng LL, Shen H, Liu L, Wang L, Li B, Fang P, Zhou Z, Li Y, Hu D. 2012. Identifying major depression using whole-brain functional connectivity: a multivariate pattern analysis. Brain. 135:1498–1507.